JACS
JOURNAL OF THE AMERICAN CHEMICAL SOCIETY
Communication
pubs.acs.org/JACS

Self-Assembly of Charged Bodipy Dyes To Form Cassettes That Display Intracomplex Electronic Energy Transfer and Accrete into Liquid Crystals

Jean-Hubert Olivier,[†] Joaquín Barberá,[‡] Effat Bahaidarah,[§] Anthony Harriman,[§] and Raymond Ziessel*[,†]

[†]Laboratoire de Chimie Organique et Spectroscopies Avancées (LCOSA), Ecole Européenne de Chimie, Polymères et Matériaux, LMSPC, UMR 7515 associé au CNRS, 25 rue Becquerel, 67087 Strasbourg Cedex 02, France

[‡]Departamento de Química Orgánica, Instituto de Ciencia de Materiales de Aragón, Universidad de Zaragoza-CSIC, 50009 Zaragoza, Spain

[§]Molecular Photonics Laboratory, School of Chemistry, Bedson Building, Newcastle University, Newcastle upon Tyne, NE1 7RU, United Kingdom

Supporting Information

ABSTRACT: Red- and blue-absorbing boron dipyrromethene dyes, bearing opposite electronic charges, associate in solution to form a 1:2 complex having a stability constant of ca. 10^{17} M^{-2}. The complex can be dismantled by addition of a large excess of tetra-*N*-butylammonium cations. The same complex displays liquid crystalline properties on heating from rt to above 150 °C, as characterized by various experimental techniques. Highly efficient electronic energy transfer from the red to the blue dye occurs in both the initial complex and the subsequent mesomorphic state.

Ionic self-assembly (ISA)[1] is a powerful technique that employs attractive electrostatic forces to organize functionalized molecular modules into nanometer-sized materials, such as nanoparticles,[2] nanoplatelets,[3] nanoblobs,[4] nanotubes,[5] composite thin films,[6] organo-gels,[7] or liquid-crystalline phases.[8] In this latter case, the hierarchical superstructure that forms around oppositely charged dye molecules is favored via secondary hydrophobic, H-bonding and/or $\pi-\pi$ interactions which help to determine the topology of the final aggregate.[9] In furtherance of this field, we now describe the self-assembly of a liquid-crystalline material that displays efficient electronic energy transfer across the emergent mesophase. This spontaneous assembly of ionic molecules into a functional liquid-crystalline phase avoids the reliance on the tedious, step-by-step evolution of covalently linked analogues and equips the aggregate with additional properties. The complementary molecular building blocks are formed from two dissimilar boron dipyrromethene (Bodipy) dyes.[10] Thus, the distyryl Bodipy core, $\mathbf{B_n}$, was selected as an energy acceptor because of its delocalized planar structure, suitable optical properties,[11] and monocationic nature. The more rigid donor, **R**,[12] is based on a conventional Bodipy dye equipped with two negative charges at the periphery. Electronic energy transfer (EET) might be expected from the red dye to the blue counterpart, provided these molecules can be brought into close proximity.

Complexes **1**–**3** were formed by way of electrostatic interactions between the sodium salt of the sulfo Bodipy, **R**, and the ammonium hexafluorophosphate salt of the distyryl-Bodipy, $\mathbf{B_n}$,[13] in *N*,*N*-dimethylformamide (DMF) at 60 °C (see Supporting Information (SI)). The 2/1 stoichiometry of the precipitated salt was confirmed by integration of the methyl singlet (**a**) at 2.68 ppm for **R** with the two methylenepropyne signals (**b**) at 4.68 ppm for $\mathbf{B_n}$ in the H NMR spectrum. The corresponding covalently linked compound, **4**, was isolated as the neutral analogue via a cross-coupling reaction, promoted by Pd(O), between the iodophenyl-bearing form of **B** and the terminal alkyne of the yellow Bodipy dye (see SI).

Chart 1. Electrostatically and Covalently Linked Bodipy Dyes Studied Herein

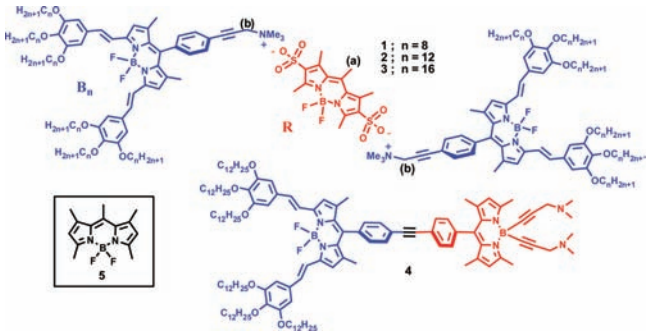

Figure 1a presents the absorption and fluorescence spectra of complex **2**. Clearly, the absorption spectrum reflects the combination of one **R** (λ_{MAX} = 513 nm, ε_{MAX} = 75 000 $M^{-1}cm^{-1}$) and two **B** dyes (λ_{MAX} = 646 nm, ε_{MAX} = 240 000 M^{-1} cm^{-1}). Note that the main absorption of **R** is shifted from 495 in isolated solution to 513 nm in the complex whereas the absorption maximum of **B** remains unchanged. Illumination at 500 nm results in strong fluorescence centered at 670 nm and for which the emission quantum yield (Φ_F) is 0.40 while the excited-singlet state lifetime (τ_s) is 4.1 ns. It is known that isolated **R** emits strongly at 520 nm but almost no (i.e., ca. 2% of the total emission) such fluorescence could be detected for the complex. This is because quantitative (i.e., >98%) energy

Received: February 2, 2012
Published: March 28, 2012

dx.doi.org/10.1021/ja3007935 | *J. Am. Chem. Soc.* 2012, 134, 6100–6103

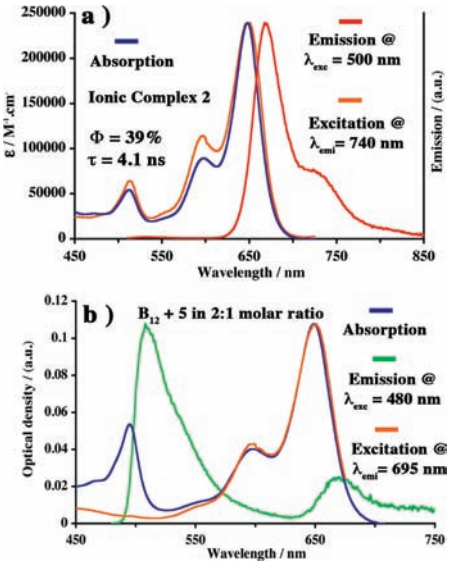

Figure 1. Absorption, fluorescence, and excitation spectra in THF, at rt, $c = 1 \times 10^{-6}$ M: (a) complex **2** (λ_{exc} = 500 nm, λ_{em} = 740 nm), (b) 2/1 mixture of $\mathbf{B_{12}}$ and dye **5** (λ_{exc} = 480 nm, λ_{em} = 695 nm).

transfer occurs from **R** to **B** within the complex, a situation confirmed by the fact that the excitation spectrum matches the absorption spectrum over the entire spectral window. Similar results were found for dyad **4**.

In the absence of anionic charges on **R**, the situation changes markedly. For example, mixing **B** and **5** in a 2:1 stoichiometry in THF results in an absorption spectrum resembling complex **2** (Figure 1b) but excitation at 480 nm results in strong fluorescence centered at 511 nm (Φ_F = 0.90: τ_s = 5.3 ns) together with the very weak emission characteristic of **B** at 670 nm (Φ_F = 0.06). This latter emission is a consequence of the direct excitation of **B** since this dye shows slight absorption at 480 nm. Moreover, the absence of EET under these conditions is indicated by the fact that the excitation spectrum recorded for emission from **B** follows the absorption spectrum of **B** free from contamination by that of **5**. At this stage, we can conclude that formation of the 2:1 complex requires electrostatic association of **B** with **R** and is manifest by the occurrence of efficient EET between the partners.

The EET event, being characteristic of the assemblage, is a useful tool by which to assess the stability of the complex. At a given concentration, the ratio (R_{DA}) of emission yields for **R** and **B** depends on the nature of the surrounding solvent and shows a general increase with decreasing static dielectric constant of the solvent (see SI). It was further noted that R_{DA} increased on dilution over the range 15 μM to ca. 20 nM, due to partial dissociation of the complex in line with Le Chateliers' Principle. Analysis of the experimental data for **2** over this range shows that the complex dissociates in two distinct steps. The first molecule of **B** is lost fairly easily ($K_1 = 3.5 \times 10^{-7}$ M), but the second **B** molecule is held more tightly ($K_2 = 7 \times 10^{-11}$ M). Interestingly, loss of the first **B** molecule is accompanied by only a slight recovery of fluorescence from **R**, which remains centered at 520 nm. It is the loss of the second molecule of **B** that restores the characteristic emission from the donor. Time-resolved fluorescence spectroscopy showed that the emission lifetime of the bis-complex is <30 ps but that of the monocomplex varies from 70 ps at high concentration to 150 ps at low concentration. This effect is attributed to the weak intermolecular association of the complex at high concentration. This latter effect is more prominent in nonpolar solvents, such as benzene, where the emission maximum for **B** moves to ca. 720 nm. It was further found that K_1 increases on cooling the solution in accord with the van't Hoff expression, giving the enthalpy change as −5.3 kJ/mol, which is attributed to an increase in the entropy of the surroundings (see SI).

In the case of **2**, it was found that R_{DA} increased progressively upon addition of tetrabutylammonium perchlorate (TBAP) in THF (Figure 2). Here, the added cation competes with **B** for

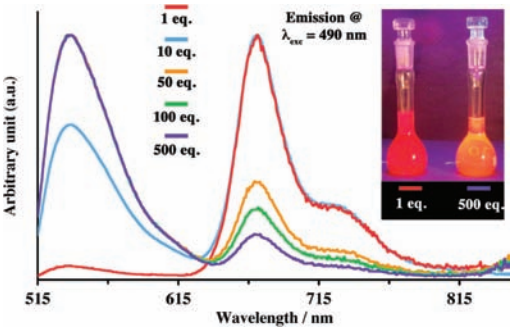

Figure 2. Fluorescence changes at rt, $c = 1 \times 10^{-6}$ M, by successive addition of TBAP in THF. λ_{exc} = 490 nm.

association to **R** and dismantles the original complex; presumably, a new ion pair is formed by way of electrostatic binding. In THF, the first **B** molecule is readily replaced by TBA+, but this has only a small effect on the fluorescence spectral profile. Fitting the titration data allows estimation of the relative binding constants as being ca. 17-fold in favor of **B**. Exchange of the more tightly bound **B** molecule demands a large excess of TBAP (e.g., >100 mol equiv for complete replacement) and fully restores emission from the donor. Data analysis is consistent with the mixed complex having a ca. 10^4-fold greater preference for **B** than TBA+. By taking due account of the fact that TBAP is likely to form a complex by way of electrostatic interactions, it follows that complexes such as **2** are stabilized by ancillary interactions.

The liquid-crystalline properties of **1**−**3** were examined by polarizing optical microscopy (POM), differential scanning calorimetry (DSC), and X-ray diffraction (XRD).[14] The results of these studies are gathered in Table 1. All complexes display comparable phase behavior with a 3D crystalline phase at rt that transforms under heating into a hexagonal columnar mesophase (Col_h), which persists on further heating to the point of thermal decomposition. On cooling the mesophase, in each case, a mesomorphic glass appears that maintains the structural characteristics of the hexagonal columnar mesophase (confirmed by XRD, see later). Crystallization is not apparent by either POM or DSC during cooling. For **1** and **2**, crystallization does not take place even on cooling to −40 °C, and therefore in the second heating and successive scans no transitions are observed. In contrast, **3** crystallizes on cooling below rt and the crystal-to-mesophase transition is observed during the second heating cycle, although at a temperature significantly lower than seen in the initial cycle (Table 1). The covalently linked dye **4** melts directly to the isotropic liquid, which partially or totally crystallizes on cooling without passing through a mesomorphic phase. X-ray patterns recorded at different temperatures confirm that **4** is crystalline below the transition to the isotropic liquid at 181 °C. A crystal-to-crystal transition takes

dx.doi.org/10.1021/ja3007935 | J. Am. Chem. Soc. 2012, 134, 6100−6103

Table 1. Thermal and X-ray Data for Compounds 1−3[a]

compd	transition temp/°C (ΔH/kJ·mol)	d_{meas} (Å) at 25 °C	d_{calc} (Å)	$hk0$	a (Å)
1	1st heating: Cr 155 (48.1) Col_h ~215 dec.	49.9	49.8	100	57.5
		28.7	28.8	110	
		24.7	24.9	200	
		19.0	18.8	210	
		4.4[b]			
2	1st heating: Cr 77 (107.6) Col_h ~210 dec.	54.2	54.5	100	62.9
		31.7	31.45	110	
		27.4	27.25	200	
		4.4[b]			
3	1st heating: Cr 85 (260.9) Col_h	55.0	55.1	100	63.6
		31.9	31.8	110	
		4.4[b]			
	1st and 2nd cooling: Col_h 12 (116.1) Cr′				
	2nd heating: Cr′ 19 (101.8) Col_h ~190 dec.				

[a]Temperature at the peak maxima; Cr, Cr′ crystalline phases; Col_h: hexagonal columnar mesophase; Iso: isotropic liquid. X-ray measurements for the cooling process. d_{meas} and d_{calc} are the measured and calculated diffraction spacing; $hk0$ is the index of the reflections of the 2D lattice of the Col_h. [b]Diffuse, broad maximum.

place at 65 °C. The lack of flexibility, the bulky dimethylaminopropyne groups at the boron center, and the nonplanar diphenylacetylene spacer in **4** hinder $\pi-\pi$ stacking between neighboring aromatic cores, thereby preventing bulk phase organization. Such flexibility and the nondirectional electrostatic interactions confirm the versatility of ISA processes.

In contrast, variable-temperature X-ray diffraction studies are consistent with formation of a columnar mesophase of hexagonal symmetry for complexes **1**−**3**; the lattice constants a calculated from the registered $hk0$ X-ray reflections at rt are given in Table 1. As expected, the magnitude of a depends on the dimensions of the molecule, increasing progressively with increasing chain length. No 001 reflections corresponding to the regular stacking of the molecules within the columnar mesophase are observed. Therefore, it appears that these complexes present a *disordered*, hexagonal columnar mesophase consistent with the absence of a planar aromatic core inherent to classical disk-like mesogens.[15]

So how do these charged compounds pack together in the mesophase so as to build the resultant columnar structure? The density, ρ, of the compounds and the number, Z, of molecules in the unit cell are related by $\rho = (M/N)/(V/Z)$: where M is the molar mass (g/mol), N is Avogadro's constant, and V refers to the unit cell volume (cm^3). The latter term can be calculated from the lattice constant ($V = (\sqrt{3}/2)a^2c$) while the density is reasonably estimated to be in the range 0.9−1 g cm^{-3}. Within these various approximations, the mean stacking distance (i.e., c) for **1**−**3** was ~4−4.5 Å on the basis of $Z = 2$. This derived separation is in line with values found for other columnar mesophases of self-organized nondisk-like molecules[9a−c,16] and is considered to be fully consistent with a scaffold consisting of stacked pairs of complexes. Such dimers would bear a total number of 24 peripheral chains able to form a disordered state surrounding the central columns. In the proposed structure, the **R** units must occupy the inner part of the dimer core and the **B** units must be located with their ammonium groups close to the sulfonate anions of **R** but with their hydrocarbon chains spreading out toward the periphery.

Interestingly, an intense, broad fluorescence profile spanning from 650 to 850 nm is observed for the columnar mesophase of **2** when dispersed on a glass slide. This latter emission is broadened significantly and red-shifted compared to that from the corresponding solution phase due to the ordering of the molecule in the thin film (Figure 3). The shape and intensity of the fluorescence profile depend on the temperature, at least over the range 20−150 °C. Since there is essentially no emission from **R** it is concluded that quantitative EET occurs in the mesophase. Indeed, mixing complex **B12** with **5** in a 2:1 stoichiometry and annealing at 150 °C leads to the appearance of dual emission at 550 and 750 nm when the film is examined at 100 °C in the bulk state (Figure 3). This set of experiments provides strong support for the idea that the complex is not dismantled at 150 °C and that the mesophase is stable at high temperature.

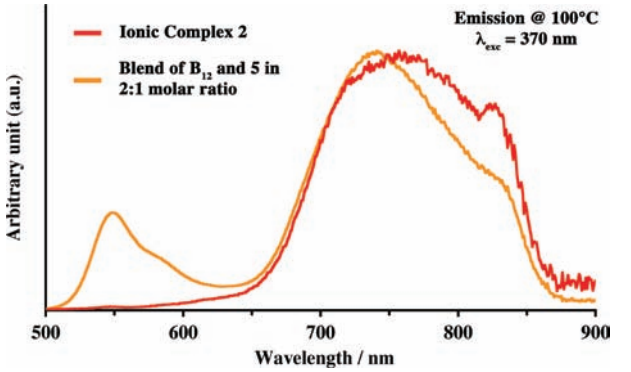

Figure 3. Fluorescence spectrum (λ_{exc} = 370 nm) of complex **2** in the columnar mesophase at 100 °C (red trace). Fluorescence spectrum (λ_{exc} = 370 nm) of complex **B12** mixed with dye **5** in a 2 to 1 mol stoichiometry in the solid state at 100 °C (orange trace).

In summary, ISA provides an attractive alternative to covalent bonding in regards to the creation of molecular entities capable of displaying highly efficacious EET. Moreover, this approach facilitates the growth of organized mesophases, under mild conditions, retaining the EET step. A further benefit of the ISA methodology is that the emergent mesophase has the potential to function as a superior light-harvesting array for silicon-based solar cells.

■ ASSOCIATED CONTENT

Supporting Information

General methods, synthetic experimental part, absorption and fluorescence spectra, NMR spectra, DSC traces, wide-angle and small-angle X-ray diffraction patterns, stability constant measurements. This material is available free of charge via the Internet at http://pubs.acs.org.

■ AUTHOR INFORMATION

Corresponding Author

ziessel@unistra.fr

Notes

The authors declare no competing financial interest.

■ ACKNOWLEDGMENTS

We thank the Centre National de la Recherche Scientifique (CNRS) and the Royal Saudi Government for financial support of this work. J.B. acknowledges the UE (FEDER funds) and the Spanish Government (CTQ2009-09030 project).

■ REFERENCES

(1) (a) Faul, C. J. J.; Antonietti, M. *Adv. Mater.* **2003**, *15*, 673−683. (b) Wu, D.; Pisula, W.; Enkelmann, V.; Feng, X.; Müllen, K. *J. Am. Chem. Soc.* **2009**, *131*, 9620−9621. (c) Tian, Y.; Martin, K. E.; Shelnutt, J. Y.-T.; Evans, L.; Busani, T.; Miller, J. E.; Medforth, C. J.; Shelnutt, J. A. *Chem. Commun.* **2011**, *47*, 6069−6071. (d) Ahmed, R.; Hsiao, M.-S.; Matsuura, Y.; Houbenov, N.; Faul, C. F. J.; Manners, I. *Soft Matter* **2011**, *7*, 10462−10471.

(2) Caruso, F.; Caruso, R.; Möhwald, H. *Science* **1998**, *282*, 1111−1114.

(3) Cassagneau, T.; Fendler, J. H.; Mallouk, T. E. *Langmuir* **2000**, *16*, 241−246.

(4) Cini, N.; Tulun, T.; Decher, G.; Ball, V. *J. Am. Chem. Soc.* **2010**, *132*, 8264−8265.

(5) Wang, Z.; Medforth, C. J.; Shelnutt, J. A. *J. Am. Chem. Soc.* **2004**, *126*, 15954−15955.

(6) Rosidian, A.; Liu, Y.; Claus, R. O. *Adv. Mater.* **1998**, *10*, 1087−1091.

(7) Zakrevskyy, Y.; Faul, C. F. J.; Guan, Y.; Stumpe, J. *Adv. Funct. Mater.* **2004**, *14*, 835−841.

(8) (a) Zhang, T.; Spitz, C.; Antonietti, M.; Faul, C. F. J. *Chem.—Eur. J.* **2005**, *11*, 1001−1009. (b) Kato, T.; Mizoshita, N.; Kishimoto, K. *Angew. Chem., Int. Ed.* **2006**, *45*, 38−68.

(9) (a) Camerel, F.; Ulrich, G.; Barbera, J.; Ziessel, R. *Chem.—Eur. J.* **2007**, *13*, 2189−2200. (b) Olivier, J.-H.; Camerel, F.; Barbera, J.; Retailleau, P.; Ziessel, R. *Chem.—Eur. J.* **2009**, *15*, 8163−8174. (c) Olivier, J.-H.; Camerel, F.; Ulrich, G.; Barbera, J.; Ziessel, R. *Chem.—Eur. J.* **2010**, *16*, 7134−7142. (d) Huang, Y.; Yan, Y.; Smarsly, B. M.; Wei, Z.; Faul, C. F. J. *J. Mater. Chem.* **2009**, *19*, 2356−2362.

(10) (a) Ziessel, R.; Ulrich, G.; Harriman, A. *New J. Chem.* **2007**, *31*, 496−501. (b) Loudet, A.; Burgess, K. *Chem. Rev.* **2007**, *107*, 4891−4932. (c) Ulrich, G.; Ziessel, R.; Harriman, A. *Angew. Chem., Int. Ed.* **2008**, *47*, 1184−1201.

(11) Hablot, D.; Harriman, A.; Ziessel, R. *Angew. Chem., Int. Ed.* **2011**, *50*, 7833−7836.

(12) Boyer, J. H.; Haag, A. M.; Sathyamoorthi, G.; Soong, M.-L.; Thangaraj, K.; Pavlopoulos, T. G. *Heteroat. Chem.* **1993**, *4*, 39−49.

(13) Olivier, J.-H.; Widmaier, J.; Ziessel, R. *Chem.—Eur. J.* **2011**, *17*, 11709−11714.

(14) (a) Yoshio, M.; Kagata, T.; Mukai, T.; Ohno, H.; Kato, T. *J. Am. Chem. Soc.* **2006**, *128*, 5570−5577. (b) Kouwer, P. H. J.; Swager, T. M. *J. Am. Chem. Soc.* **2007**, *129*, 14042−14052. (c) Stepien, M.; Donnio, B.; Sessler, J. L. *Angew. Chem., Int. Ed.* **2007**, *46*, 1431−1435. (d) Laschat, S.; Baro, A.; Giesselmann, F.; Hägele, C.; Scalia, G.; Judele, R.; Kapatsina, E.; Sauer, S.; Scheivogel; Tosoni, M. *Angew. Chem., Int. Ed.* **2007**, *46*, 4832−4887. (e) Santoro, A.; Prokhorrov; Kozhevnikov, V. N.; Whitwood, A. C.; Donnio, B.; Williams, J.-A.; Gareth; Bruce, D. W. *J. Am. Chem. Soc.* **2011**, *133*, 5248−5251.

(15) (a) Levelut, A. M. *J. Chim. Phys.* **1983**, *80*, 149−161. (b) Donnio, B.; Guillon, D.; Deschenaux, R.; Bruce, D. W. *Compr. Coord. Chem.* **2003**, *7*, 357−627. (c) Kumar, S. *Chem. Soc. Rev.* **2006**, *35*, 83−109. (d) Laschat, S.; Baro, A.; Steinke, N.; Giesselman, F.; Hägele, C.; Scalia, G.; Judele, R.; Kapatsina, E.; Sauer, S.; Schreivogel, A.; Tosoni, M. *Angew. Chem., Int. Ed.* **2008**, *47*, 2754−2787.

(16) Shimogaki, T.; Dei, S.; Ohta, K.; Matsumoto, A. *J. Mater. Chem.* **2011**, *21*, 10730−10737.